unimportant in d^8–d^8 complexes,[2–6] as the spacing between $^3(d\sigma^*p\sigma)$ and the $d\delta p\sigma$ excited states is relatively large (energy gap > 4800 cm^{-1}).

Acknowledgment. We thank L. S. Fox and J. R. Winkler for measuring the transient difference spectrum of $Pd_2(dppm)_3$ at Brookhaven National Laboratory. This research was supported by National Science Foundation Grant CHE84-19828. P.D.H. acknowledges the Government of Canada for a NSERC-NATO postdoctoral fellowship.

Contribution from the Department of Chemistry,
University of Leuven, Celestijnenlaan 200F, 3030 Leuven, Belgium

Electronic Spectra of the d^6 Binary Carbonyl Complexes $Mn(CO)_6^+$, $Cr(CO)_6$, and $V(CO)_6^-$: An ab Initio Analysis

K. Pierloot, J. Verhulst, P. Verbeke, and L. G. Vanquickenborne*

Received December 28, 1988

The UV–visible spectra of the isoelectronic series $Mn(CO)_6^+$, $Cr(CO)_6$, and $V(CO)_6^-$ have been reinvestigated by using the Hartree–Fock–Roothaan method. The calculations do confirm the classical assignment of the two intense absorption peaks as MLCT transitions. For the weak bands, however, an alternative assignment has been proposed. It is essentially based on the observation that the calculated spectrochemical strength $10Dq$ *increases* in the order $Mn(CO)_6^+ < Cr(CO)_6 < V(CO)_6^-$; this result is in conflict with earlier assignments.

I. Introduction

The electronic spectra of the neutral and ionic d^6 binary carbonyls have been known for a long time. In 1963, Gray and Beach were the first to report the vapor-phase spectra for the hexacarbonyls of the group VIB metals Cr–Mo–W.[1] In a more recent paper, the same authors[2] also include the ionic species $Mn(CO)_6^+$, $V(CO)_6^-$, and $Re(CO)_6^+$.

As one would expect, the electronic spectra of these series of complexes are very similar. Each one of them contains two intense absorption bands, which were identified as metal-to-ligand charge-transfer transitions ($d\pi \rightarrow L\pi^*$), in addition to a number of weaker bands, assigned as d–d transitions.

The assignment of the two larger peaks in the spectra is straightforward, since in these d^6 species only two metal-to-ligand excitations are orbitally allowed, namely $^1A_{1g}(t_{2g}^6) \rightarrow {}^1T_{1u}(t_{2g}^5t_{1u}^1)$ and the $^1A_{1g}(t_{2g}^6) \rightarrow {}^1T_{1u}(t_{2g}^5t_{2u}^1)$ transition. The weaker bands present a more difficult problem, and a number of slightly different assignments have been proposed.[1–6] Eventually however, the original assignment of Beach and Gray became rather widely accepted.[7] It is shown in Table I for the isoelectronic series $V(CO)_6^-$, $Cr(CO)_6$, and $Mn(CO)_6^+$.

As can be seen from Table I, in each spectrum five bands were identified. For $V(CO)_6^-$ and $Cr(CO)_6$ the energetic sequence of the two strong and three weaker bands is identical, and therefore, in both cases, the strong bands were assigned as MLCT transitions, the weak signal between these bands was assigned as a ligand field transition to $^1T_{2g}$, and the two lowest weak bands were assigned as vibrational components of the ligand field transition to $^1T_{1g}$. The latter assignment was partially substantiated by the fact that the separation between the two signals nearly equals the CO stretching frequence.[2]

The $Mn(CO)_6^+$ spectrum is slightly different. The $^1T_{2g}$ band between the two MLCT signals turned out to be undetectable, but instead of a new weak signal appeared below the two $^1T_{1g}$ bands. The latter signal was assigned as a spin-forbidden ligand field transition to $^3T_{1g}$.

Table I. Electronic Spectral data for $V(CO)_6^-$, $Cr(CO)_6$, and $Mn(CO)_6^+$ in Acetonitrile Solution and Assignment According to Reference 2

complex	$\bar{\nu}$, cm^{-1}	ϵ, cm^{-1}	10^2f	assignment
$[n\text{-}B_4N][V(CO)_6]$	$\{$23 200	300	0.28	vibrational components
	25 100	1 640	2.0	of $^1A_{1g} \rightarrow {}^1T_{1g}$ (d–d)
	28 400	6 240	8.0	$^1A_{1g} \rightarrow {}^1T_{1u}(d\text{–}t_{1u})$
	~31 100	3 300	~3.2	$^1A_{1g} \rightarrow {}^1T_{2g}(d\text{–}d)$
	37 550	60 900	120	$^1A_{1g} \rightarrow {}^1T_{1u}(d\text{–}t_{2u})$
	41 200	21 200	29	
	43 700	13 700	16	
$Cr(CO)_6$	$\{$29 500	700	0.61	vibrational components
	31 550	2 670	3.3	of $^1A_{1g} \rightarrow {}^1T_{1g}(d\text{–}d)$
	35 700	13 100	24	$^1A_{1g} \rightarrow {}^1T_{1u}(d\text{–}t_{1u})$
	38 850	3 500	4.0	$^1A_{1g} \rightarrow {}^1T_{2g}(d\text{–}d)$
	43 600	85 100	227	$^1A_{1g} \rightarrow {}^1T_{1u}(d\text{–}t_{2u})$
	>50 000			
$[Mn(CO)_6][BF_4]$	~33 250	600	1	$^1A_{1g} \rightarrow {}^3T_{1g}(d\text{–}d)$
	$\{$~37 300	1 100	2	vibrational components
	~39 600	2 200	2	of $^1A_{1g} \rightarrow {}^1T_{1g}(d\text{–}d)$
	44 500	16 000	34	$^1A_{1g} \rightarrow {}^1T_{1u}(d\text{–}t_{1u})$
	49 900	27 000	61	$^1A_{1g} \rightarrow {}^1T_{1u}(d\text{–}t_{2u})$

According to these assignments, the different transitions all move to higher energies in the order $V(CO)_6^- < Cr(CO)_6 < Mn(CO)_6^+$. For the M → L charge-transfer bands, this behavior is to be expected since the d-orbital energy must decrease, and therefore, the π^*–d energy difference must increase as the charge on the central metal becomes more positive. The simultaneous increase of the ligand field transition energies however is less obvious. Starting from the assignments in Table I, the following $10Dq$ values were calculated for the three complexes:[2]

$$V(CO)_6^-:\ 10Dq = 25\,500\ \text{cm}^{-1}$$

$$Cr(CO)_6:\ 10Dq = 32\,200\ \text{cm}^{-1}$$

$$Mn(CO)_6^+:\ 10Dq = 41\,050\ \text{cm}^{-1}$$

Now according to the traditional MO picture, the ligand field separation $10Dq$ between the e_g and t_{2g} orbitals in these carbonyl complexes arises from two mechanisms: on the one hand, the CO to metal σ-donation causes a destabilization of the e_g orbitals, while on the other hand the t_{2g} orbitals are stabilized due to π-back-donation into the empty π^*(CO) orbitals. During the last decades

---

(1) Gray, H. B.; Beach, N. A. *J. Am. Chem. Soc.* **1963**, *85*, 2922.
(2) Beach, N. A.; Gray, H. B. *J. Am. Chem. Soc.* **1968**, *90*, 5713.
(3) Abel, E. W.; McLean, R. A. N.; Tyfield, S. P.; Braterman, P. S.; Walker, A. P.; Hendra, P. J. *J. Mol. Spectrosc.* **1969**, *30*, 29.
(4) Wrighton, M. S.; Handeli, D. I.; Morse, D. L. *Inorg. Chem.* **1976**, *15*, 434.
(5) Wrighton, M. S.; Morse, D. L.; Gray, H. B.; Ottesen, D. K. *J. Am. Chem. Soc.* **1976**, *98*, 1111.
(6) Lever, A. B. P.; Ozin, G. A. *Inorg. Chem.* **1977**, *16*, 2012.
(7) Lever, A. B. P. *Inorganic Electronic Spectroscopy*, 2nd ed.; Elsevier: Amsterdam, 1984.

0020-1669/89/1328-3059$01.50/0

special attention has been given to the importance of both bonding types.[8,9] Experimental[10] as well as theoretical studies[11] have clearly shown that the π-back-bonding is much more important in $V(CO)_6^-$ than it is in $Mn(CO)_6^+$. Qualitatively, this can be explained by the same argument that was used to explain the shift of the M → L charge-transfer bands: the increasing π^*–d-orbital energy separation with increasing positive charge on the central metal must necessarily lead to a decrease in the interaction between these orbitals, and thus to a decreasing stabilization of the t_{2g} orbital. An increasing value of $10Dq$ in the order $V(CO)_6^- < Cr(CO)_6 < Mn(CO)_6^+$ would imply that this decreasing stabilization of the t_{2g} shell is counteracted by an even larger increase in the destabilization of the e_g shell, due to σ bonding. We are not aware of any evidence for such a strong variation of the σ-bonding capabilities of CO within the isoelectronic series. In view of these considerations, the increasing values of $10Dq$ in the order $V(CO)_6^- < Cr(CO)_6 < Mn(CO)_6^+$, based on the Beach and Gray assignment of their electronic spectra, and hence this assignment itself, seem rather unlikely.

Furthermore, even the assignment of the two intense peaks as M → L charge-transfer transitions has recently been questioned.[12] On the basis of the study of solvent effects on the electronic spectrum of the related $Cr(\eta^6\text{-}C_6H_6)_2$ complex, it was argued that the two intense peaks in the $Cr(CO)_6$ spectrum rather should be assigned as metal d–s and d–p Rydberg transitions.

In view of the above considerations, a reinvestigation of the electronic spectra of these complexes seems necessary. It is the purpose of this paper to present a number of SCF calculations on the relevant spectra, including the ligand field and M → L charge-transfer transitions, as well as the metal 3d–4s and 3d–4p excitations. Due to the inherent lack of correlation in the SCF method, the calculations presented here are necessarily preliminary, and it is certainly not our intention to obtain an exact reproduction of the experimental transition energies. Rather we will focus on the qualitative aspects of the spectra: from a comparison of the calculated band positions for the three complexes, we will be able to offer an alternative assignment of the experimental spectra, reflecting the role played by the metal charge on the bonding characteristics. Furthermore, a number of ground-state density difference plots will be presented, which will further illustrate the relative role played by σ-donation and π-back-donation of the CO ligands in this isoelectronic series of complexes.

II. Calculational Details

The SCF calculations have been carried out within the framework of Roothaan's RHF open-shell formalism.[13] The geometry of the three molecules was taken to be perfectly octahedral. The average values of the bond lengths of the $Cr(CO)_6$ complex, as determined by means of the X–N method,[14] are 1.140 Å for C–O and 1.914 Å for Cr–C. The experimental bond lengths of the $V(CO)_6^-$ complex, 1.146 Å for C–O and 1.931 Å for V–C,[15] are only slightly different. For the $Mn(CO)_6^+$ complex, no experimental bond lengths are known. We decided to perform all calculations using the *same* internuclear distances for the three complexes, namely 1.140 Å for C–O and 1.914 Å for M–C (the distances for the Cr complex). The use of only one set of internuclear distances will allow us to substract the density plots of the three molecules, thus facilitating a comparison of their σ- and π-characteristics (see section III).

Table II. Properties of the Irreducible Representations of Octahedral $M(CO)_6$ Complexes

irreducible representation	M orbitals	CO orbitals	irreducible representation	M orbitals	CO orbitals
a_{1g}	s	σ	t_{2g}	d	π
e_g	d	σ	t_{1u}	p	σ, π
t_{1g}		π	t_{2u}		π

For the metal atoms we used a (15s 11p 6d/11s 8p 4d) basis, as detailed elsewhere.[16,17] The ligand atoms were described by the Huzinaga–Dunning basis set (9s 5p/5s 3p).[18,19] The combination of these two sets should constitute a well-balanced basis.[20] For the ground state of $Cr(CO)_6$ for example, the total energy is calculated at −1719.4277 hartrees. This is more than 2 hartrees lower than the value of −1717.2739 hartrees that resulted from an extensive CI calculation[21] using a smaller basis set. The ground-state energy of $V(CO)_6^-$ was calculated at −1619.0934 hartrees, while for $Mn(CO)_6^+$, we found an energy of −1825.6493 hartrees.

Table II shows the association of the different metal and CO orbitals within the irreducible representations of the octahedral point group. Each of the three complexes under consideration is characterized by the low-spin ground-state configuration $(8a_{1g})^2(5e_g)^4(1t_{1g})^6(8t_{1u})^6(1t_{2u})^6(2t_{2g})^6$, resulting in a $^1A_{1g}$ ground state. From this ground state, only transitions to $^1T_{1u}$ are fully allowed.

In order to investigate the assignment of the electronic spectra proposed in the literature, we carried out SCF calculations on the following excited states.

Ligand Field Transitions (d–d): $2t_{2g} \rightarrow 6e_g$. The first excited ligand field configuration $(2t_{2g})^5(6e_g)^1$ leads to the states $^3T_{1g}$, $^3T_{2g}$, $^1T_{1g}$, and $^1T_{2g}$. The ligand field expressions for the energy of these states, relative to the $^1A_{1g}$ ground state are given by

$$\begin{aligned} E(^3T_{1g}) - E(^1A_{1g}) &= 10Dq - 3C \\ E(^3T_{2g}) - E(^1A_{1g}) &= 10Dq + 8B - 3C \\ E(^1T_{1g}) - E(^1A_{1g}) &= 10Dq - C \\ E(^1T_{2g}) - E(^1A_{1g}) &= 10Dq + 16B - C \end{aligned} \tag{1}$$

By fitting the SCF energies of the four states to the above ligand field expressions, we will be able to calculate an SCF estimate of the ligand field parameters $10Dq$, B, and C.

MLCT Transitions (d–π^*): $2t_{2g} \rightarrow 9t_{1u}$ and $2t_{2g} \rightarrow 2t_{2u}$. Of the four π^*(CO) orbitals $2t_{1g}$, $3t_{2g}$, $9t_{1u}$, and $2t_{2u}$, only the last two are relevant, since a transition from $2t_{2g}$ to the two ungerade orbitals generates a $^1T_{1u}$ state. We also calculated the corresponding $^3T_{1u}$ states, since the spin-forbidden transitions to these states are expected to have about the same intensity as the ligand field transitions and can thus not be excluded a priori from the spectra.[22]

d–s and d–p Transitions: $2t_{2g} \rightarrow 9a_{1g}$ and $2t_{2g} \rightarrow 10t_{1u}$. The $2t_{2g} \rightarrow 9a_{1g}$ transition leads to a $^1T_{2g}$ state. For the $2t_{2g} \rightarrow 10t_{1u}$ transition again only the $^1T_{1u}$ state was calculated.[22,23]

---

(8) (a) Baerends, E. J.; Ros, P. *Mol. Phys.* **1975**, *30*, 1735. (b) Demuynck, J.; Veillard, A. *Theor. Chim. Acta* **1973**, *28*, 241. (c) Pearson, R. G. *Inorg. Chem.* **1984**, *23*, 4675. (d) Arratia-Perez, R.; Yang, C. J. *J. Chem. Phys.* **1985**, *83*, 4005. (e) Koutecky, J.; Pacchioni, G.; Fantucci, P. *Chem. Phys.* **1985**, *99*, 87. (f) Baerends, E. J.; Rozendaal, A. *NATO ASI Ser. Ser. C* **1986**, *176*, 159. (g) Bauschlicher, C. W.; Bagus, P. S. *J. Chem. Phys.* **1984**, *81*, 5889.

(9) (a) Johnson, J. B.; Klemperer, W. G. *J. Am. Chem. Soc.* **1977**, *99*, 7132. (b) Sherwood, D. E., Jr.; Hall, H. B. *Inorg. Chem.* **1980**, *19*, 1805. (c) Sherwood, D. E., Jr.; Hall, H. B. *Inorg. Chem.* **1983**, *22*, 93.

(10) (a) Jones, L. H. *J. Mol. Spectrosc.* **1962**, *8*, 105. (b) Jones, L. H. *J. Mol. Spectrosc.* **1962**, *9*, 130. (c) Cotton, F. A.; Kraihanzel, C. S. *J. Am. Chem. Soc.* **1962**, *84*, 4432.

(11) Caulton, K. G.; Fenske, R. F. *Inorg. Chem.* **1968**, *7*, 1273.

(12) Wittmann, G. T. W.; Krynauw, G. N.; Lotz, S.; Ludwig, W. *J. Organomet. Chem.* **1985**, *293*, C33.

(13) Roothaan, C. C. J. *Rev. Mod. Phys.* **1960**, *32*, 179.

(14) Rees, B.; Mitschler, A. *J. Am. Chem. Soc.* **1976**, *98*, 7918.

(15) Wilson, R. D.; Bau, R. *J. Am. Chem. Soc.* **1974**, *96*, 7601.

(16) Vanquickenborne, L. G.; Verhulst, J. *J. Am. Chem. Soc.* **1983**, *105*, 1769.

(17) Vanquickenborne, L. G.; Haspeslagh, L.; Hendrickx, M.; Verhulst, J. *Inorg. Chem.* **1984**, *23*, 1677.

(18) Dunning, T. H. *J. Chem. Phys.* **1970**, *53*, 2823.

(19) Huzinaga, S. J. *J. Chem. Phys.* **1965**, *42*, 1293.

(20) Vanquickenborne, L. G.; Verhulst, J.; Coussens, B.; Hendrickx, M.; Pierloot, K. *J. Mol. Struct* (*THEOCHEM*) **1987**, *153*, 227.

(21) Moncrieff, D.; Ford, P. C.; Hillier, I. H.; Saunders, V. R. *J. Chem. Soc., Chem. Commun.* **1983**, 1108.

(22) Due to the appearance in the energy expression of the T_{1u} states of repulsion integrals that are not of the J or K type, these states cannot be calculated directly within Roothaan's formalism. The calculated energy given in Table III is therefore the average energy of the T_{1u} and the corresponding T_{2u} states. The energy separation between these two states is always very small. In order to verify this, we also calculated the energy of the $T_{1u}(d\text{–}\pi^*)$ states, using the orbitals of the T_{1u}–T_{2u} state average. The result is only very slightly different from the values given in Table III. As an example, for $Cr(CO)_6$, the $^1A_{1g} \rightarrow {}^1T_{1u}(d\text{–}t_{1u})$ transition is now calculated at 33 738 cm^{-1} (+298 cm^{-1}), and the $^1A_{1g} \rightarrow {}^1T_{1u}(d\text{–}t_{2u})$ transition at 42 684 cm^{-1} (+120 cm^{-1}).

(23) For the sake of simplicity, the $^1A_{1g} \rightarrow {}^3T_{2g}$(d–s) and $^1A_{1g} \rightarrow {}^3T_{1u}$(d–p) transitions were not included in Table III and in Figure 1. Due to the diffuseness of the 4s and 4p orbitals, the energy separation between these triplet transitions and the corresponding singlet transitions is very small. Thus for $Cr(CO)_6$, the $^1A_{1g} \rightarrow {}^3T_{2g}$(d–s) transition is calculated only 247 cm^{-1} below the $^1A_{1g} \rightarrow {}^1T_{2g}$(d–s) transition, while for the d–p transition, the energy separation between the $^1A_{1g} \rightarrow {}^3T_{1u}$ and the $^1A_{1g} \rightarrow {}^1T_{1u}$ transitions is 898 cm^{-1}.

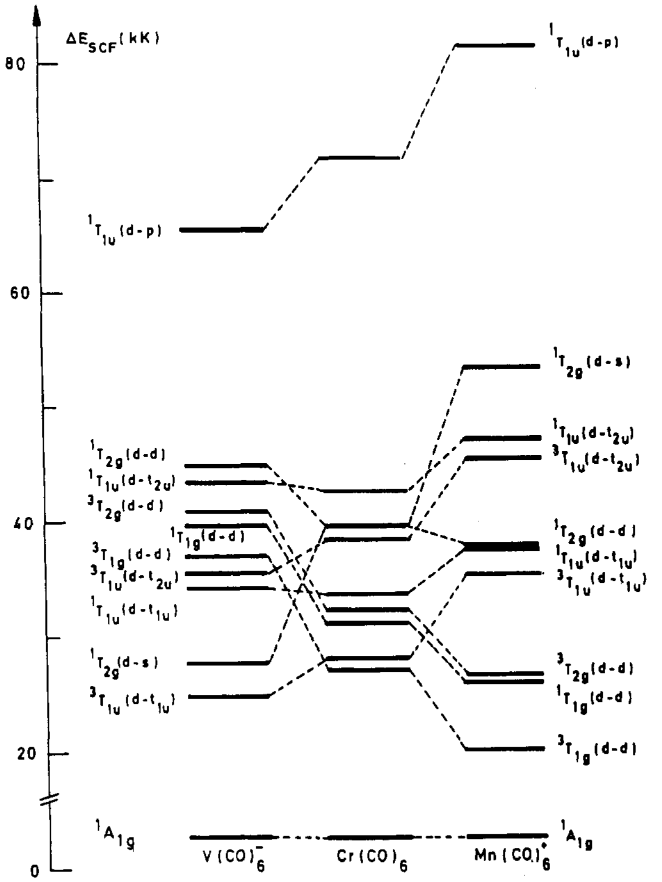

Figure 1. Correlation diagram, connecting the SCF energies of the different excited states of $V(CO)_6^-$, $Cr(CO)_6$, and $Mn(CO)_6^+$. The ground states of the different molecules are given zero energy.

III. Results and Discussion

The SCF energies of the different excited states, relative to the $^1A_{1g}$ ground state, are given in Table III. Figure 1 shows an energy-level diagram, connecting the corresponding excited states for the three complexes. On the basis of our SCF results, we proposed an alternative assignment of the experimental energy bands, given in the third column of Table III. The last column shows the relative deviation of the calculated energy values from the corresponding experimental transition energies.

When comparing our assignment with the original Beach and Gray assignment from Table I, the following points should be stressed.

1. The identification of the two largest peaks as M → L charge-transfer bands is maintained. For the $Cr(CO)_6$ complex, the agreement between the experimental and the calculated transition energies is excellent. For the other two complexes, the deviation is larger. This may be due partly to the fact that the internuclear distances used in the calculation of these complexes differ somewhat from the experimental bond lengths. But more important, the fact that the higher coordination spheres are not included in the calculation will result in larger errors for the charged complexes. Indeed, since an M → L transition necessarily involves a flow of negative charge to the outside of the molecule, the presence of the second coordination sphere will, depending on its charge, lead to a stabilization or destabilization of the excited charge-transfer states relative to the ground state. This is reflected by the sign of the deviations in Table III. In the case of $Mn(CO)_6^+$, the transition energies are calculated too low, due to the neglect of the anions in the second coordination sphere. For $V(CO)_6^-$ on the other hand, the situation is reversed: the presence of the cations in the second coordination sphere tends to stabilize the charge-transfer states, which are thus calculated too high.

Due to the different sign of the deviations in $V(CO)_6^-$ and $Mn(CO)_6^+$, the experimentally observed increase of the charge-transfer energy with increasing positive charge on the central metal is not fully reproduced by the theoretical results. As can be seen from Figure 1, the calculated transition energy in fact slightly decreases when going from $V(CO)_6^-$ to $Cr(CO)_6$. Yet, in view of the above considerations, it is clear that the two intense absorption bands indeed have to be assigned as M → L charge-transfer transitions in the three cases and not, as proposed in ref 12, as d–s or d–p transitions.

Table III. SCF Energies of the Different Excited States Relative to the $^1A_{1g}$ Ground State, and Assignment of the Experimental Spectral Data of the Octahedral Complexes $V(CO)_6^-$, $Cr(CO)_6$, and $Mn(CO)_6^+$

transition	ΔE_{SCF}, cm^{-1}	$\bar{\nu}_{exp}$,[a] cm^{-1}	dev, %
	A. $V(CO)_6^-$		
$^3T_{1u}$(d–t_{1u})	25 359	23 200	9.3
$^1T_{2g}$(d–s)	27 883	25 100	11.1
$^1T_{1u}$(d–t_{1u})	33 889	28 400	19.3
$^3T_{1u}$(d–t_{2u})	35 164	~31 100	13.1
$^3T_{1g}$(d–d)	37 180		
$^1T_{1g}$(d–d)	39 570		
$^3T_{2g}$(d–d)	40 919		
$^1T_{1u}$(d–t_{2u})	43 585	37 550	16.2
$^1T_{2g}$(d–d)	44 962		
		41 200	
		43 700	
$^1T_{1u}$(d–p)	65 462		
	B. $Cr(CO)_6$		
$^3T_{1g}$(d–d)	27 274		
$^3T_{1u}$(d–t_{1u})	28 499	29 500	−3.4
$^1T_{1g}$(d–d)	31 097	31 550	−1.4
$^3T_{2g}$(d–d)	32 297		
$^1T_{1u}$(d–t_{1u})	33 440	35 700	−6.3
$^3T_{1u}$(d–t_{2u})	38 105	38 850	−1.9 to +2.0
$^1T_{2g}$(d–d)	39 596		
$^1T_{2g}$(d–s)	39 631		
$^1T_{1u}$(d–t_{2u})	42 561	43 600	−2.4
$^1T_{1u}$(d–p)	71 910		
	C. $Mn(CO)_6^+$		
$^3T_{1g}$(d–d)	19 987		
$^1T_{1g}$(d–d)	25 661		
$^3T_{2g}$(d–d)	26 608		
		~33 250	
$^3T_{1u}$(d–t_{1u})	35 728	~37 300	−4.2
$^1T_{2g}$(d–d)	38 043	~39 600	−3.9
$^1T_{1u}$(d–t_{1u})	37 874	44 500	−14.9
$^3T_{1u}$(d–t_{2u})	45 294		
$^1T_{1u}$(d–t_{2u})	46 971	49 900	−5.9
$^1T_{2g}$(d–s)	53 293		
$^1T_{1u}$(d–p)	82 008		

[a] New assignment.

2. The d–s transition does show up in the spectrum, however, at least for $V(CO)_6^-$ and $Cr(CO)_6$. Actually, in discussions of the electronic spectrum of most first-row transition metal complexes, this transition does not have to be considered. Indeed, due to the positive charge on the central metal the corresponding transition energy is usually too large. As can be seen from Table III, this is also the case for $Mn(CO)_6^+$. In $Cr(CO)_6$, however, the central chromium is formally neutral, while in $V(CO)_6^-$ the vanadium has a formal charge of −1. As Figure 1 shows, this results in a sharp decrease of the transition energy of the $^1A_{1g} \rightarrow {}^1T_{2g}$(d–s) and the $^1A_{1g} \rightarrow {}^1T_{1u}$(d–p) transitions.

While the d–p transition energy remains too large to be detected, even for $V(CO)_6^-$, the d–s transition clearly falls into the visible UV region for $Cr(CO)_6$ and $V(CO)_6^-$: in $Cr(CO)_6$, the $^1T_{2g}$(d–d) and $^1T_{2g}$(d–s) states are virtually degenerate,[24] while in $V(CO)_6^-$, the d–s transition even lies below all ligand field transitions. Therefore we believe that the weak, low-energy band at 25 100 cm^{-1} in the electronic spectrum of $V(CO)_6^-$ should be assigned as the $^1A_{1g} \rightarrow {}^1T_{2g}$(d–s) transition and not as the $^1A_{1g} \rightarrow {}^1T_{1g}$(d–d)

---

[24] As can be seen from Table III, in the case of $Cr(CO)_6$, the transitions to the $^1T_{1u}$(d–t_{2u}), $^1T_{2g}$(d–d), and $^1T_{2g}$(d–s) states are all calculated at an energy that is very close to the experimental band at 38 850 cm^{-1}, which can therefore correspond to any of these three transitions.

Table IV. SCF Estimate of the Ligand Field Parameter $10Dq$ and the Racah Parameters B and C, Calculated by Fitting the SCF Energies of the Different $(2t_{2g})^5(6e_g)^1$ States to the Ligand Field Expressions Given in Eq 1 (cm^{-1})

param	$V(CO)_6^-$	$Cr(CO)_6$	$Mn(CO)_6^+$
$10Dq$, cm^{-1}	40 414	32 852	28 557
B, cm^{-1}	356	541	774
C, cm^{-1}	930	1744	2773
B_{ion},[a] cm^{-1}	536	756	988
C_{ion},[a] cm^{-1}	1874	2711	3601
B/B_{ion}	0.66	0.72	0.78
C/C_{ion}	0.50	0.64	0.77

[a] B_{ion} and C_{ion} represent the free-ion SCF values.

transition (see Table I). The latter transition is calculated to be about 15 000 cm^{-1} higher. The deviation of 11.1% between the calculated d–s transition energy and the experimental energy band (see Table III) again can be attributed to the neglect of the second coordination sphere: since the 4s orbital is a very diffuse orbital, the d–s transition will involve a transfer of negative charge to the outside of the molecule.

3. The SCF calculations do confirm the Beach and Gray assignment of the weak $Cr(CO)_6$ bands at 31 550 and 38 850 cm^{-1} as ligand field transitions to $^1T_{1g}$ and $^1T_{2g}$.[24] As for the charge-transfer transitions, the agreement between the calculated and the experimental transition energies is remarkably good. For the other two complexes, however, the SCF results strongly suggest that Gray's assignment of the ligand field bands should be modified. As stated in the Introduction, according to this assignment the ligand field transitions move to higher energy in the order $V(CO)_6^- < Cr(CO)_6 < Mn(CO)_6^+$. Now from Figure 1 it is clear that this sequence should actually be reversed: the calculated transition energies are much higher for $V(CO)_6^-$ than for $Mn(CO)_6^+$.

Table IV shows the value of the ligand field parameters $10Dq$, B, and C that were obtained by fitting the SCF energies of both singlet and triplet ligand field transitions to eq 1. The $10Dq$ values follow of course the same trend as the transition energies themselves, or

$$10Dq(V(CO)_6^-) > 10Dq(Cr(CO)_6) > 10Dq(Mn(CO)_6^+) \quad (2)$$

Also included in Table IV are the free-ion SCF values of the Racah parameters B and C. By comparing the free-ion values to the values that were obtained for the complexes, one can see that the trend of eq 2 is reflected in the repulsion parameters as well: the nephelauxetic ratio increases from $V(CO)_6^-$ to $Mn(CO)_6^+$, corresponding to a decrease of the overlap between the 3d orbitals and the CO ligand orbitals.

As stated in the Introduction, the $10Dq$ sequence of eq 2 must be traced back to the strongly decreasing π-back-donation to the CO ligands as the charge on the central metal ion becomes more positive. This is further illustrated in Figures 2 and 3. Figure 2 shows the ground-state electron density change in the three complexes due to complexation. For $Cr(CO)_6$, a similar plot was presented in ref 9c. Figure 2 clearly illustrates the classical picture of the CO ligand as a σ-donor and π-acceptor: on the one hand, electron density is transferred from the metal t_{2g} orbitals into the C and O p orbitals, while on the other hand one can see a negative charge flow from the CO σ orbitals into the metal e_g orbitals. A comparison of this plot for the three complexes shows how the π-back-donation decreases in the order $V^- > Cr > Mn^+$. The O p orbital seems to be particularly affected: the negative charge transfer into this orbital has almost completely disappeared in $Mn(CO)_6^+$. A more detailed picture of the situation is presented in Figure 3. Here, the total densities of $V(CO)_6^-$ and $Cr(CO)_6$ on the one hand and of $Cr(CO)_6$ and $Mn(CO)_6^+$ on the other hand are directly substracted from each other. Since the differences in bonding characteristics between the different complexes are somewhat obscured by changes in the metal core functions, we decided to include only the valence orbitals in this figure. As can be seen now, the strongly increasing π-back-donation when going from Mn^+ to Cr and from Cr to V^- is accompanied by a slightly

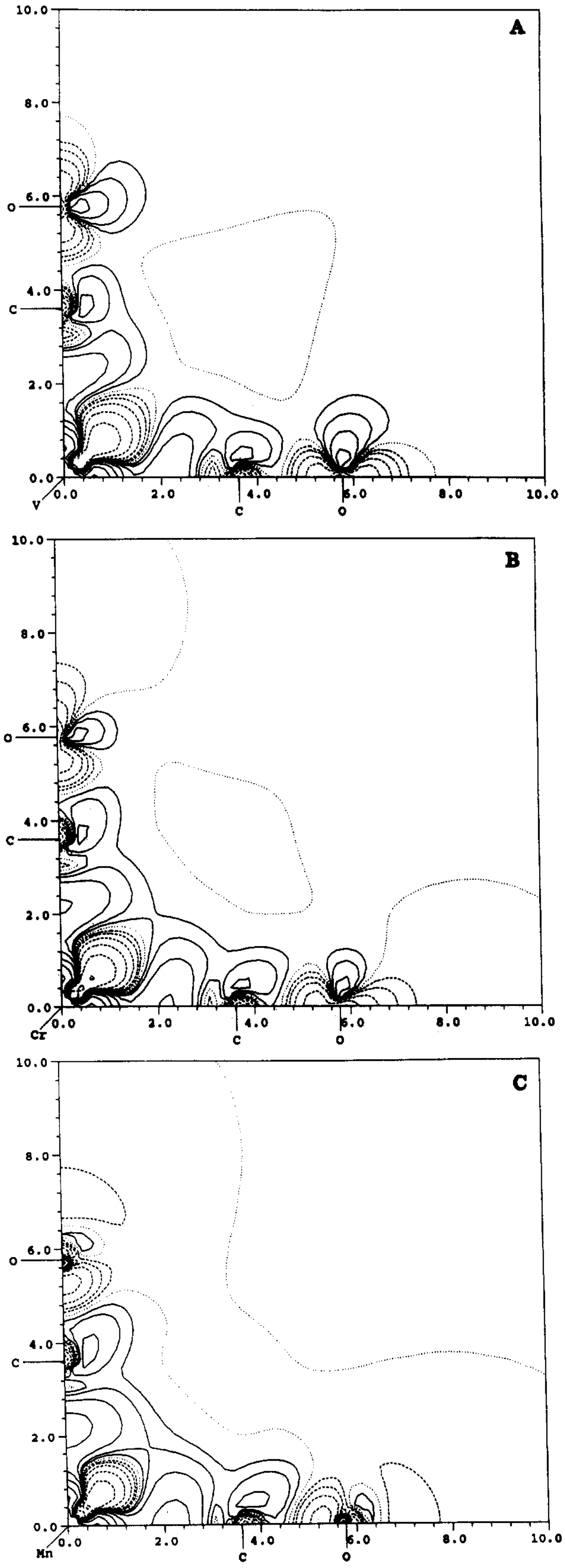

Figure 2. Total density difference plot $\Delta\rho = \rho(\text{complex}) - \rho(\text{metal–ligand system})$ for the $^1A_{1g}$ ground state of $V(CO)_6^-$ (A), $Cr(CO)_6$ (B), and $Mn(CO)_6^+$ (C). The plots describe the electronic density shifts in the *xy* plane upon bond formation. The separated metal–ligand system consists of the metal, calculated in the $^1A_{1g}(t_{2g}^6)$ state, plus six CO ligands, all noninteracting but located at the internuclear distances in the complex. All distances are in atomic units. Full contours correspond to an electron density increase and dashed contours to an electron density decrease, while at the dotted lines $\Delta\rho = 0$. The values of the $\Delta\rho$ contours are ±0.0025, ±0.005, ±0.01, ±0.02, ±0.04, ±0.08, and ±0.16 au^{-3}.

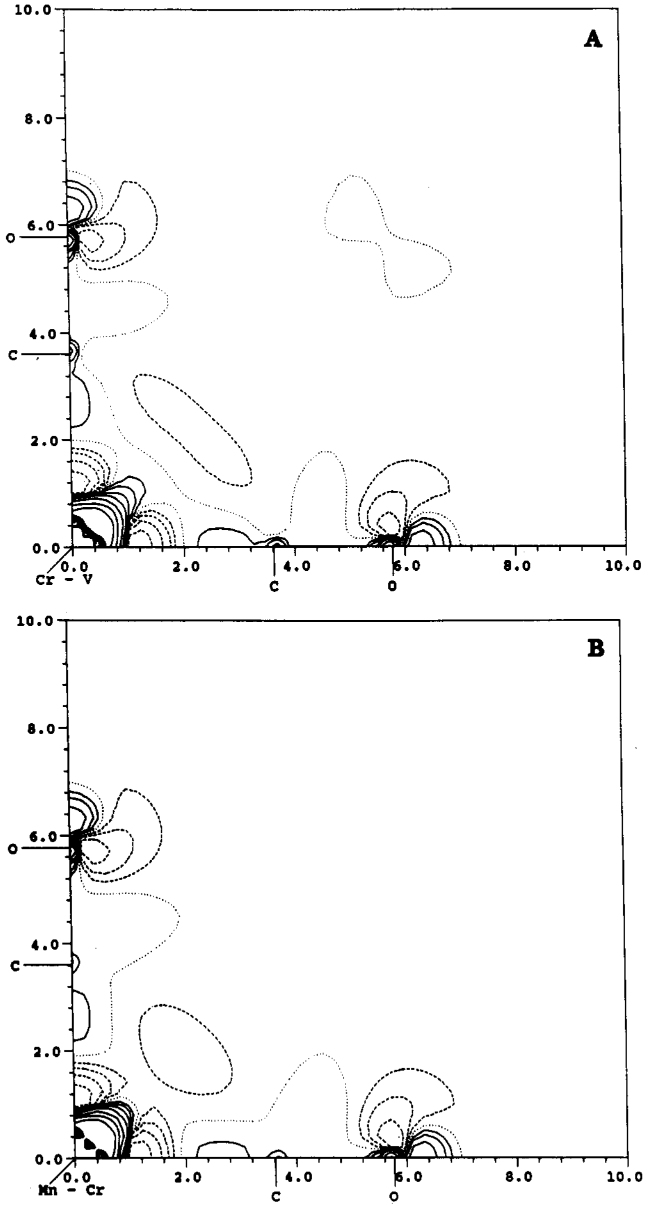

Figure 3. Density difference plot $\Delta\rho_v = \rho_v(\text{complex 1}) - \rho_v(\text{complex 2})$ describing the electronic density shift within the valence orbitals (6–8 a_{1g}, 3–5 e_g, $1t_{1g}$, 5–8t_{1u}, 1–2t_{2g}) in the xy plane: (A) $\rho_v(Cr(CO)_6) - \rho_v(V(CO)_6^-)$; (B) $\rho_v(Mn(CO)_6^+) - \rho_v(Cr(CO)_6)$. All distances are in atomic units. Full contours correspond to an electron-density increase and dashed contours to an electron-density decrease, while at the dotted lines $\Delta\rho_v = 0$. The values of the $\Delta\rho_v$ contours are ±0.0025, ±0.005, ±0.01, ±0.02, ±0.04, ±0.08, and ±0.16 au^{-3}.

increasing σ-donation. So it is clear that, within this isoelectronic series, both the σ-donating and π-accepting capabilities of the CO ligands increase as the charge on the central metal becomes more negative, although the π-effect is much more important. Furthermore, it is also clear that the spectroscopic properties of the complexes, notably the position of the ligand field bands, are related to their ground-state properties: both effects, the increasing π-back-bonding and the increasing σ-donation, will make a positive contribution to the strongly increasing ligand field strength when going from $Mn(CO)_6^+$ to $V(CO)_6^-$.

4. In view of these considerations, an alternative assignation of the weak bands in the spectrum of $Mn(CO)_6^+$ and $V(CO)_6^-$ has been proposed. As can be seen from Table III, no ligand field transitions have been assigned in the spectrum of $V(CO)_6^-$. The transition to $^1T_{1g}$ is probably obscured by the close-lying, very intense $^1A_{1g} \rightarrow {}^1T_{1u}(d-t_{2u})$ transition. The transition to $^1T_{2g}$ was calculated at an energy that is close to those of the bands at 41 200 and 43 700 cm^{-1}, but the intensity of these bands (see Table I) is too high to make them a possible candidate for a ligand field transition. As suggested in ref 3, both high-energy bands in the spectrum of $V(CO)_6^-$ should probably be assigned as higher, orbitally forbidden M → L charge-transfer transitions, hiding the $^1A_{1g} \rightarrow {}^1T_{2g}$(d–d) transition. As for $Mn(CO)_6^+$, our calculations show that the band at 39 600 cm^{-1} is indeed a ligand field transition, only not to $^1T_{1g}$, as suggested by Beach and Gray, but to $^1T_{2g}$. The $^1A_{1g} \rightarrow {}^1T_{1g}$ transition is calculated too low to be responsible for the very weak band at 33 250 cm^{-1}.

Table III further shows that, according to our new assignment, in each of the three spectra at least one band is identified as a spin-forbidden M → L charge-transfer transition. More specifically, the bands that were originally identified by Beach and Gray as the lower vibrational components of the $^1A_{1g} \rightarrow {}^1T_{1g}$(d–d) transition (at 23 200 cm^{-1} for $V(CO)_6^-$, 29 500 cm^{-1} for $Cr(CO)_6$, and 37 300 cm^{-1} for $Mn(CO)_6^+$) now are assigned as $^1A_{1g} \rightarrow {}^3T_{1u}(d-t_{1u})$ transitions. Furthermore, the $^1A_{1g} \rightarrow {}^3T_{1u}(d-t_{2u})$ transition is observed in the spectrum of $V(CO)_6^-$ at 31 100 cm^{-1}.[24]

The following arguments are in favor of our assignment:

(i) As can be seen from Table I, the intensity of the bands under consideration is very low, as is expected for spin-forbidden transitions. More important however is the fact that these intensities are proportional to the intensities of the corresponding singlet transitions. Thus in the $V(CO)_6^-$ spectrum, the intensity of the band at 31 100 cm^{-1} is much larger than that for the band at 23 200 cm^{-1} in accordance with the relative intensities of the corresponding singlet transitions, at 37 500 and 28 400 cm^{-1}, respectively.

(ii) As Table III shows, the sign of the deviations is in the same sense as for the other bands in the spectra: negative for $Mn(CO)_6^+$, negative but smaller for $Cr(CO)_6$, and positive for $V(CO)_6^-$.

The most important observation regarding the triplet transitions however is the fact that they are very well separated from the corresponding singlet transitions, so that they can actually be observed in the spectra. This is another indication of the large amount of π-back-bonding in the complexes under consideration. Due to the large overlap between the metal d and the CO π orbitals, the $2t_{2g}$ orbital contains a fairly large amount of ligand character. This in turn results in a large overlap between this orbital and the π^* $9t_{1u}$ and $2t_{2u}$ orbitals. Therefore, the proper exchange integrals and thus the spin pairing energy are much larger in carbonyl complexes than in other, less covalent complexes of the first-row transition metals. As can be seen from Table III, the energy separation between two corresponding singlet and triplet M → L transitions strongly decreases in the order $V(CO)_6^- > Cr(CO)_6 > Mn(CO)_6^+$, in accordance with the strongly decreasing π-back-bonding in the same order.

IV. Conclusion

To summarize our findings, we note that the electronic spectra of the d^6 binary carbonyl complexes can be reproduced with a reasonable accuracy by (large basis set) SCF results. For $Cr(CO)_6$ the agreement between the calculated and experimental transition energies is excellent, while the sign of the deviation for the other two (charged) complexes conforms with the fact that the calculations did not include any higher coordination spheres.

Our calculations do confirm the classical assignment of the two most intense bands in the spectra of M → L charge-transfer transitions. For the weaker bands, however, we propose an alternative assignment, taking into account the following points:

(i) The ligand field transitions all move to higher energy in the order $Mn(CO)_6^+ < Cr(CO)_6 < V(CO)_6^-$, due to the large increase in π-back-bonding and the smaller increase in σ-donation of the CO ligands as the negative charge increases. *This interpretation of the spectra strongly deviates from the assignments proposed so far.*

(ii) Due to the low formal charge of the metal in $Cr(CO)_6$ and $V(CO)_6^-$, the d–s transition is situated in the UV region and therefore has to be taken into account.

(iii) The extensive π-back-bonding in these complexes is also responsible for the considerable energy separation between the singlet and triplet charge-transfer bands; as a consequence, triplet charge-transfer bands are observed in the three spectra.